Available online at www.sciencedirect.com
SCIENCE DIRECT®
Journal of Solid State Chemistry 177 (2004) 3174–3182
JOURNAL OF SOLID STATE CHEMISTRY
http://elsevier.com/locate/jssc

Location of type B carbonate ion in type A–B carbonate apatite synthesized at high pressure

Michael E. Fleet* and Xiaoyang Liu

Department of Earth Sciences, University of Western Ontario, London, Ont., Canada N6A 5B7

Received 28 August 2003; received in revised form 9 December 2003; accepted 2 April 2004

Available online 15 July 2004

Abstract

The structure of a complex, disordered type A–B carbonate apatite (CAp) of approximate composition $Ca_{10}(PO_4)_{6-y}(CO_3)_{x+(3/2)y}(OH)_{2-2x}$, x–0.7, y–0.6, synthesized at 3 GPa, 1400°C has been determined using single-crystal X-ray diffraction and FTIR spectroscopy at room temperature and pressure. Crystal data are: hexagonal, space group $P6_3/m$, $Z = 1$; $a = 9.5143(3)$, $c = 6.8821(2)$ Å, $V = 539.5$ Å^3, and $R = 0.025$. There are three structural locations for the carbonate ion. The channel carbonate is mainly in the closed vertical configuration of the $P\bar{3}$ structure, with two of its oxygen atoms close to the c-axis (A1 carbonate; IR bands at 1541 and 1449 cm^{-1}), but subordinate amounts are also located in an open vertical configuration (A2 carbonate; IR bands at 1563 and 1506 cm^{-1}). The type B carbonate ion is located close to the sloping faces of the PO_4 tetrahedron (IR bands at 1474 and 1406 cm^{-1}), confirming earlier inferences from polarized IR spectra.

Keywords: Carbonate apatite; CAp; Type B (phosphate) Carbonate ion; Bone; Enamel; High-pressure phosphates

1. Introduction

The structural roles of the carbonate ion in hydroxylapatite ($Ca_{10}(PO_4)_6(OH)_2$; OHAp; space group $P6_3/m$, [1–6]) have been studied extensively by X-ray diffraction, chemical analyses, infrared (IR) and Raman spectroscopy, and proton and ^{13}C NMR spectroscopy [7–14]. As reviewed in Ref. [14], there is general agreement that the carbonate ion can substitute both for OH in the apatite channel (type A CAp) and for the phosphate ion (type B CAp), and that these different structural roles result in characteristic IR signatures: type A carbonate having a doublet band at about 1545 and 1450 cm^{-1} (asymmetric stretching vibration, v_3) and a singlet band at 880 cm^{-1} (out-of-plane bending vibration, v_2), and type B having these bands at about 1455, 1410 and 875 cm^{-1}, respectively. Elliott [7] deduced from polarized IR spectra that the type A carbonate ion in enamel was oriented with its plane approximately parallel to the c-axis and the type B carbonate ion in francolite (C-FAp) occupied a sloping tetrahedral face of the substituted phosphate ion. Suetsugu et al. [12] reported that the space group of type A CAp was $P\bar{6}$, and the equilateral triangular cluster of the channel carbonate ion was bisected by the c-axis (the "open" configuration [14]). On the other hand, study of carbonate apatite (CAp) synthesized at high pressure, but having an IR signature similar to that of type A CAp in bone and enamel, revealed space group $P\bar{3}$ [14]; the type A carbonate ion was ordered along the apatite channel at $z = 0.5$, and oriented with two of its oxygen atoms close to the c-axis (the "closed" configuration). X-ray powder diffraction Rietveld structure refinement of a synthetic Ca-deficient C–OHAp (space group $P6_3/m$) suggested that the type B carbonate ion occupied the vertical face of the substituted phosphate ion [13]. In this study, crystals of type A–B CAp are grown at high pressure in the presence of excess calcium carbonate and investigated by single-crystal X-ray diffraction and FTIR spectroscopy. It is shown that the structure of type A–B CAp is complex, and likely composite; the type B carbonate ion is located close to the sloping faces of the PO_4 group, and a second

*Corresponding author. Fax: +519-661-3198.
E-mail address: mfleet@uwo.ca (M.E. Fleet).

0022-4596/$ - see front matter © 2004 Elsevier Inc. All rights reserved.
doi:10.1016/j.jssc.2004.04.002

(stuffed) orientation of the channel carbonate ion is identified.

2. Experimental procedures

The experimental procedures, including synthesis at 3 GPa in an end-loaded piston-cylinder apparatus, FTIR spectroscopy using a Nicolet Nexus 670 FTIR spectrometer, and single-crystal measurements at room temperature and pressure with a Nonius Kappa CCD diffractometer and graphite-monochromatized Mo$K\alpha$ X-radiation (50 kV, 32 mA, $\gamma = 0.71069$ Å), were similar to the earlier study [14]. In this study, the starting mixture contained a higher proportion of $CaCO_3$; $Ca_2P_2O_7$, CaO and $CaCO_3$ being present in the molar ratio (8/3):(8/3):2. The high-pressure synthesis experiment (PC55) yielded crystals of CAp (up to 300 μm in maximum diameter) and minor calcite. Powder X-ray diffraction (XRD) measurements on the unwashed CAp (made with a Rigaku D/MAX-B system; Co$K\alpha$ X-radiation) resulted in a hexagonal unit cell with $a = 9.521(1)$, $c = 6.8870(9)$ Å. Aliquots of the products of PC55 were supported on platinum foil and annealed in air at 1000°C for time intervals ranging from 15 min to 24 h. Powder XRD on the samples annealed for 12 and 24 h showed change in peak intensity and peak positions of CAp and a high proportion of X-ray amorphous material. The COLLECT Nonius software was used for unit-cell refinement and data collection for selected single crystals, and the reflection data were processed with SORTAV-COLLECT and SHELXTL/PC [15]. Structure refinements were made with LINEX77 (State University of New York at Buffalo), using scattering factors for neutral atomic species and values of f' and f'' from Tables 2.2A and 2.3.1, respectively, of the *International Tables for X-ray Crystallography* [16]. Relevant experimental details are given in Table 1, final parameters in Table 2, and selected bond distances and angles in Table 3; the average structure of the high-pressure product is depicted in Figs. 1 and 2.

3. Results and discussion

In the previous study [14], the starting composition for the high-pressure experiments contained $Ca_2P_2O_7$, CaO and $CaCO_3$ in the molar ratio 3:3:1, and resulted in single-phase carbonate-rich type A carbonated apatites belonging to the ideal composition series $Ca_{10}(PO_4)_6[(CO_3)_x(OH)_{2-2x}]$, with $x \geqslant 0.5$. Although the type A carbonate ion in the $P\bar{3}$ structure was ordered along the apatite channel at $z = 0.5$, the partial occupancy of oxygen positions and smearing of the electron density associated with the carbon position pointed to disordering of the carbonate atoms by rotoinversion about the c-axis, as required by the $P\bar{3}$ symmetry. The high proportion of $CaCO_3$ in the starting

Table 1
Experimental details

Carbonate apatite	High-pressure crystal xt376	Annealed crystal xt383	Annealed crystal xt377
Experiment	PC55	PC55-1000-15	PC55-1000-12
Pressure	3 GPa[a]	1 bar	1 bar
Temperature (°C)	1400	1000	1000
Time (h)	5.5	15 min	12
Crystal size (mm^3)	$0.09 \times 0.10 \times 0.06$	$0.07 \times 0.07 \times 0.04$	$0.11 \times 0.11 \times 0.035$
Crystal shape	square prism	tablet	platelet
a (Å)	9.5143(3)	9.4931(4)	9.4716(4)
c (Å)	6.8821(2)	6.8888(5)	6.8968(3)
Space group	$P6_3/m$	$P6_3/m$	$P6_3/m$
Formula weight	1020.3	1017.0	1019.7
Density (g/cm^3)	3.140	3.141	3.160
Reflections—unique	579	565	675
Number, with ($I < 3\sigma_{(I)}$)	242	386	383
$R_{(I)}$	0.025	0.035	0.030
$R_{(I),w}$	0.041	0.046	0.043
Refined parameters	57	57	57
μ (cm^{-1})	28.4	28.4	28.6
R	0.024	0.031	0.030
R_w	0.031	0.039	0.059
S	1.06	1.58	3.19
g ($\times 10^4$)	0.5(1)	0.4(1)	0.4(2)
$\Delta\rho$ (e $Å^{-3}$) (+)	0.35	0.44	0.48
(−)	0.42	0.44	0.40

[a] X-ray diffraction measurements were made at room temperature and pressure.

Table 2
Positional and isotropic thermal parameters (Å^2) ($B_{eq} = 4/3\Sigma_i\Sigma_j\beta_{ij}a_i \cdot a_j$)

	Site occupancy	x	y	z	B[a], B_{eq}
PC55: xt376					
Ca(1)	1.0	2/3	1/3	0.0024(1)	1.42(3)
Ca(2)	1.0	0.98994(8)	0.25099(7)	1/4	1.82(2)
P	0.927(3)	0.37173(9)	0.4024(1)	1/4	1.28(2)
O(1)	1.0	0.4847(2)	0.3320(3)	1/4	1.70(4)
O(2)	1.0	0.4663(3)	0.5857(3)	1/4	3.41(6)
O(3)	0.963	0.2617(3)	0.3480(4)	0.0734(3)	4.15(5)
O(H)	0.118(5)	0.017(2)	0	1/4	1.97[a]
C	0.32(1)	0	0	0	1.97[a]
O(A11)	0.096(3)	0.036(2)	0.014(4)	0.652(2)	1.97[a]
O(A12)	0.058(4)	0.940(3)	0.123(3)	0.529(4)	1.97[a]
O(A2)	0.095(4)	0.904(2)	0.010(2)	0.457(2)	1.97[a]
O(B3)	0.048(4)	0.360(4)	0.421(4)	0.460(6)	1.97[a]
PC55-1000-15: xt383					
Ca(1)	1.0	2/3	1/3	0.0021(3)	1.89(9)
Ca(2)	1.0	0.9890(2)	0.2509(2)	1/4	2.13(6)
P	0.941(7)	0.3706(3)	0.4010(3)	1/4	1.53(8)
O(1)	1.0	0.4840(5)	0.3310(5)	1/4	1.8(1)
O(2)	1.0	0.4656(6)	0.5848(6)	1/4	3.6(2)
O(3)	0.971	0.2590(8)	0.3441(8)	0.0726(8)	4.4(1)
O(H)	0.072(6)	0.013(7)	0	0.22	1.97[a]
C	0.32(3)	0	0	0	1.97[a]
O(A11)	0.116(8)	0.054(4)	0.012(8)	0.636(7)	1.97[a]
O(A12)	0.052(9)	0.93(1)	0.11(1)	0.55(1)	1.97[a]
O(A2)	0.05(1)	0.91(1)	0.03(2)	0.49(2)	1.97[a]
O(B3)	0.07(1)	0.342(8)	0.411(8)	0.45(1)	1.97[a]
PC55-1000-12: xt377					
Ca(1)	1.0	2/3	1/3	0.0021(2)	1.51(9)
Ca(2)	1.0	0.9894(2)	0.2489(2)	1/4	1.96(5)
P	0.940(6)	0.3714(3)	0.4016(3)	1/4	1.25(6)
O(1)	1.0	0.4847(6)	0.3303(6)	1/4	1.5(1)
O(2)	1.0	0.4662(7)	0.5858(7)	1/4	3.4(1)
O(3)	0.970	0.2595(8)	0.3441(9)	0.0752(7)	3.9(1)
O(H)	0.14(2)	0	0	0.22	1.97[a]
C	0.33(4)	0	0	0	1.97[a]
O(A11)	0.117(8)	0.041(5)	0.01(1)	0.657(6)	1.97[a]
O(A12)	0.058(8)	0.939(8)	0.115(9)	0.552(9)	1.97[a]
O(A2)	0.046(9)	0.94(1)	0.04(1)	0.45(1)	1.97[a]
O(B3)	0.06(1)	0.337(9)	0.41(1)	0.47(1)	1.97[a]

[a] B not refined.

Table 3
Selected bond distances (Å) and angles (deg)

	PC55 xt376	PC55-1000-15 xt383	PC55-1000-12 xt377
Ca(1)–O(1) ×3	2.425(1)	2.426(3)	2.418(3)
Ca(1)–O(2)^{I} ×3	2.487(2)	2.484(4)	2.481(4)
Ca(1)–O(3)^{I} ×3	2.804(3)	2.824(6)	2.823(7)
Mean	2.572	2.578	2.574
Ca(2)–O(1)^{II}	2.719(2)	2.695(4)	2.694(5)
Ca(2)–O(2)^{III}	2.332(2)	2.334(5)	2.340(6)
Ca(2)–O(3)^{IV} ×2	2.575(2)	2.565(6)	2.551(7)
Ca(2)–O(3)^{V} ×2	2.359(2)	2.344(5)	2.367(4)
Mean	2.486	2.474	2.478
Ca(2)–O(H)[a]	2.4373(6)	2.445(2)	2.419(2)
P–O(1)	1.525(2)	1.522(4)	1.526(5)
P–O(2)	1.510(2)	1.512(6)	1.511(6)
P–O(3) ×2	1.516(2)	1.528(5)	1.515(5)
Mean	1.517	1.523	1.517
O(1)–P–O(2)	111.3(1)	111.1(3)	111.6(3)
O(1)–P–O(3) ×2	111.39(7)	111.3(2)	111.2(2)
O(2)–P–O(3) ×2	107.9(1)	108.4(3)	108.7(3)
O(3)–P–O(3)^{VI}	106.8(2)	106.2(5)	105.4(6)

Notes: (I) $1-x$, $1-y$, $-z$; (II) $1-y$, $x-y$, z; (III) $1-x+y$, $1-x$, z; (IV) $1+x$, y, z; (V) $1+x-y$, x, $-z$; (VI) x, y, $1/2-z$.
[a] O(H) on c axis.

composition for the present high-pressure experiment (PC55) exceeded the theoretical upper limit of 1.0 for the formula amount of x. Therefore, type B carbonate was expected in the product CAp, as well as type A. There are several options for charge balancing the partial substitution of PO_4^{3-} by CO_3^{2-} in apatites, including, vacancies or Na at Ca positions, dehydroxylation of residual OH, and carbonate in channel positions. Charge compensation by additional carbonate ions in channel sites may be represented by the following ideal substitution schemes and corresponding solid solution formulae:

$$[^{A2}CO_3 + {}^{B}CO_3 = OH + PO_4], \quad (1a)$$

$$Ca_{10}(PO_4)_{6-y}(CO_3)_y[(CO_3)_{x+y}(OH)_{2-2x-y}] \quad (1b)$$

and

$$[^{A2}CO_3 + 2{}^{B}CO_3 = {}^{A2}\square + 2PO_4], \quad (2a)$$

$$Ca_{10}(PO_4)_{6-y}(CO_3)_y[(CO_3)_{x+(1/2)y}(OH)_{2-2x}]. \quad (2b)$$

In each of these substitution schemes, the charge-compensating carbonate ion occupies a stuffed apatite channel location, which we presently label "A2"; the channel location of the carbonate ion in the $P\bar{3}$ structure is now labelled "A1", and represents the substitution $[CO_3 + \square = 2OH]$.

Experiment PC55 yielded CAp and minor admixed and intergrown calcite. These products were characterized by powder X-ray diffraction, optical petrography and FTIR spectroscopy. The FTIR spectrum of the bulk product has a prominent complex of bands in the asymmetric stretching region of the carbonate ion (ν_3) consistent with a relatively high content of carbonate (Fig. 3). A very weak broad peak at $-3570\,cm^{-1}$ indicated only minor OH in apatite channel sites. The individual carbonate asymmetric stretching bands appear to be associated with calcite (singlet at $1406\,cm^{-1}$), type B carbonate (doublet of the high-frequency shoulder to the $1453\,cm^{-1}$ band and band at $1406\,cm^{-1}$), type A1 carbonate (doublet of bands at 1541 and $1453\,cm^{-1}$), and type A2 carbonate (doublet of bands at 1563 and $1506\,cm^{-1}$) [9,12,14,17–22]. There is

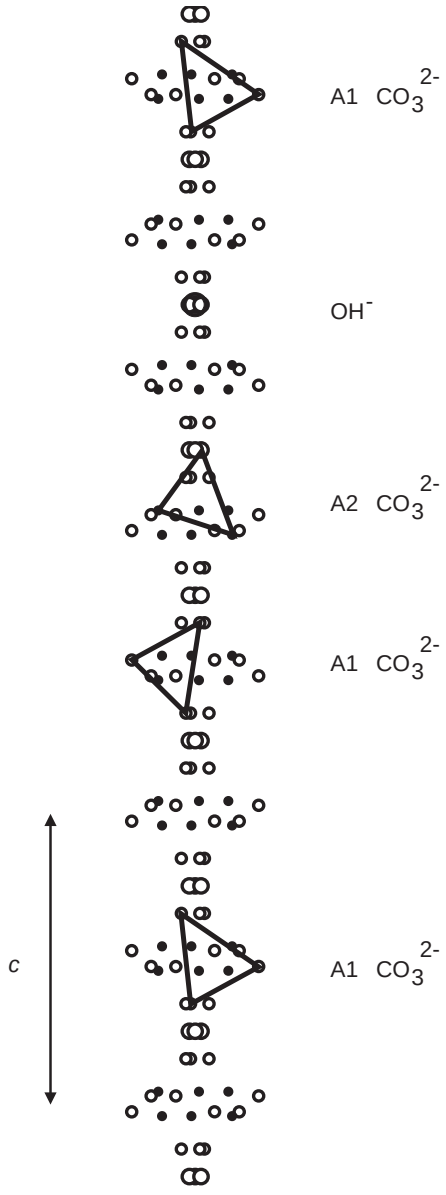

Fig. 1. Average structure within the *c*-axis channel of type A–B CAp revealed by single-crystal X-ray diffraction at room temperature and pressure, and represented by multiplicity of partially occupied carbonate oxygen atom and O(H) positions. All of the carbonate oxygen atoms are in general positions and, therefore, disordered with a multiplicity of twelve. Triangles and large circle show a possible locally ordered arrangement of four carbonate ions and one hydroxyl ion over an interval of four unit-cell repeats along the channel: small open circles are oxygen atoms of type A1 carbonate; small solid circles are oxygen atoms of type A2 carbonate; medium open circles represent the third type A2 oxygen and O(H).

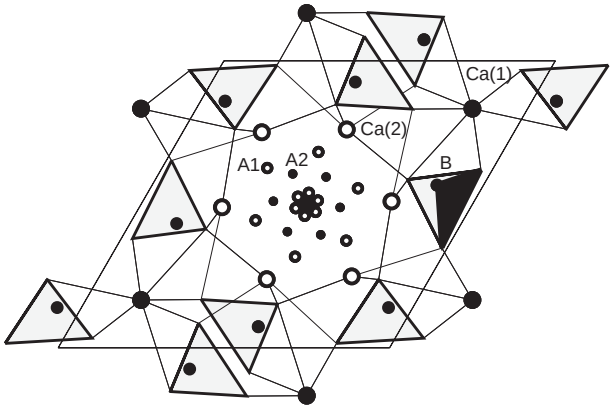

Fig. 2. The average crystal structure of type A–B CAp synthesized at 3 GPa, in *c*-axis projection, showing multiplicity of disordered carbonate oxygen and O(H) atoms. A possible type B carbonate ion (dark shaded) is located close to a sloping face of a PO_4 tetrahedron and formed from one O(3B) atom (medium solid circle) and unresolved oxygen atoms close to O(1) and O(2): small open circles are A1 oxygen atoms; small solid circles are A2 oxygen atoms.

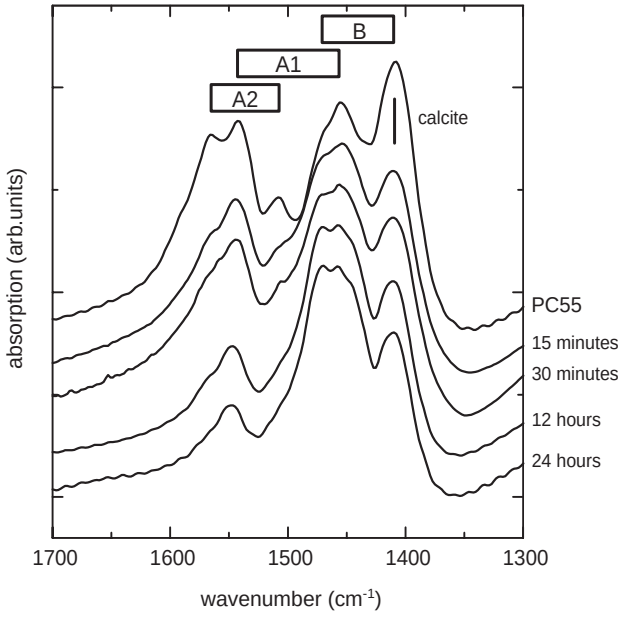

Fig. 3. FTIR spectra of carbonate-rich CAp synthesized at 3 GPa (PC55) and annealed at 1000°C for intervals of 15 and 30 min and 12 and 24 h, identifying bands due to asymmetric stretching of carbonate ions (v_3), and assigned to types B, A1 and A2 carbonate, and calcite: B is carbonate replacing phosphate; A1 is channel carbonate in closed configuration; A2 is channel carbonate in the open configuration and located in a stuffed channel position.

some ambiguity in defining the high-frequency band of the type B doublet, due to overlap with the low-frequency band of the type A1 doublet, and a case could be made for reversing the present assignments of these two peaks. Indeed, review of the literature showed that precise IR peak positions for the carbonate ion in apatite do vary, sometimes significantly [9]. The low- and high-frequency bands of the types A1 and B doublets correspond, respectively, to the v_{3a} and v_{3b} vibrations of literature studies; for both doublets, v_{3a} is the symmetric mode with transition moment parallel to a C–O bond and v_{3b} is the antisymmetric mode with its transition moment perpendicular to the same C–O bond [21].

The spectral region for asymmetric stretching of the carbonate ion in PC55 CAp has been peak fitted with Gaussian distributions using programme BGAUSS [23] (Table 4). The high-frequency features were poorly fitted by this simple scheme, and it was found necessary to introduce an additional Gaussian peak at 1597 cm^{-1}, amounting to ~9% of the total v_3 absorption. Convergence of the least-squares refinement was achieved by fixing bandwidths for the apatite carbonate ions, as well as all parameters for the calcite singlet band (at 1409 cm^{-1}) and the Gaussian peak at 1597 cm^{-1}. The best estimates of band positions for the apatite carbonate ions are obtained by using both the observed and fitted FTIR spectra; giving 1474 and 1406 cm^{-1} for type B, 1541 and 1449 cm^{-1} for type A1, and 1563 and 1506 cm^{-1} for type A2 carbonate. A weak band near 1500 cm^{-1} has previously been attributed to minor type A carbonate in type B CAp [19,20]. Also, we note that bands near 1508 and 1563 cm^{-1} appear to be weakly present in the IR spectrum of type A–B CAp synthesized at 0.55 kbar under Ar gas with excess $CaCO_3$ reagent [11]. The fitted FTIR spectrum suggests that type B, type A1 and type A2 carbonate ions are present in PC55 CAp in the approximate ratio of 0.9:1.0:0.6 (Table 4).

The location of the v_{3b} band of the type A2 carbonate doublet remains ill defined in the fitted spectrum. More generally, the present fitting procedure underestimates the contribution of type A2 carbonate to PC55 CAp; note that the formula amounts of type A2 carbonate ion deduced from the FTIR spectra in Table 4 are consistently lower than the corresponding X-ray structure values. The high-frequency spectral features, in particular, were poorly fitted, due to the complex nature of the spectra, limitations in the fitting model, fitting procedure, and BGAUSS, and inadequate background correction. The v_3 region of the IR spectrum of CAp of complex composition typically has a saw-tooth profile, rising abruptly from the background on the low-frequency side and fading into the background on the high-frequency side (e.g. Refs. [6,9–11,18–20,24–27]). Although vibrational bands are theoretically Lorentzian, in practice a variety of factors, including instrumental and substitutional broadening, lead to a band shape which closely approximates a skewed Gaussian distribution [28]. A Lorentzian peak shape would better account for the high-frequency features of the asymmetric stretching region of PC55 CAp, but neither a Lorentzian nor a Voigtian profile would adequately describe the low-frequency (v_{3a}) band of the type B doublet (Fig. 3). The simple Gaussian peak shape presently adopted appeared to be adequate for qualitative and semi-quantitative interpretation of the spectral features, although it clearly could not account for all absorption associated with each of the seven main bands. Further interpretation of the FTIR spectra using theoretical models based on symmetry analysis and

Table 4
Fitted FTIR spectra and formula amounts of carbonate

	High-pressure crystal xt376 PC55			Annealed crystal xt383 PC55-1000-15[1]			Annealed crystal xt377 PC55-1000-12[2]		
Fitted FTIR spectra									
Band	Position (cm^{-1})	Width[a] (cm^{-1})	Peak area	Position (cm^{-1})	Width[a] (cm^{-1})	Peak area	Position (cm^{-1})	Width[a] (cm^{-1})	Peak area
Type A1 doublet	1449	32	7.3	1447	34	8.5	1447	34	26.2
	1540	30	7.5	1541	34	7.0	1546	34	14.2
Type A2 doublet	1507	28	4.6	1508	30	3.2	1508	28	8.3
	1569	32	6.2	1571	30	2.8	1575	28	3.9
Type B doublet	1408	32	6.7	1408	38	9.6	1408	34	23.4
	1474	30	6.3	1476	38	9.8	1476	34	26.4
Calcite[a]	1409	56	8.9	1402	50	1.6	1407	40	0.0
Formula amounts									
Carbonate ion	Type A1	Type A2	Type B	Type A1	Type A2	Type B	Type A1	Type A2	Type B
FTIR spectra	(0.69)	0.51	0.61	(0.62)	0.24	0.71	(0.70)	0.22	0.63
X-ray structure	0.69	0.57	0.57	0.62	0.32	0.82	0.70	0.28	0.76

Notes: (1) Annealed for 15 min at 1000°C; (2) annealed for 12 h at 1000°C.
(0.69) Dependent value.
[a] Not refined.

minimum energy configurations was beyond the scope of the present study, and may not have been too meaningful, in view of the complex disordering of the carbonate ion in PC55 CAp deduced from the X-ray structure analysis (below).

We attempted to improve resolution in the ν_{3a} region of the type B carbonate ion by decarbonating the admixed and intergrown calcite at 1000°C. Interference from the calcite band (at 1400–1410 cm^{-1}) was markedly reduced after annealing for 15 min and eliminated after 12 h (Fig. 3; Table 4). However, composition and structural changes also occurred concomitantly in the CAp. The changes most evident in the FTIR spectra were diminution in the intensity of the type A2 doublet and a slight strengthening of the type B doublet. These changes point to preferential loss of type A2 channel carbonate to the atmosphere during annealing, along with some reorganization of the residual carbonate in the CAp structure. Note that the apparent asymmetry in the peak areas of the types A1 and A2 doublets of the sample annealed for 12 h reflects the difficulty in fitting the high-frequency region of the FTIR spectrum. The response of CAp synthesized at high pressure to annealing in air may be contrasted with that of CAp prepared by reaction of $CaCO_3$ and triammonium phosphate solution at ~100°C, which showed progressive movement of carbonate ion from type B sites to type A1 sites for annealing temperatures up to 900°C [29].

Single-crystal X-ray diffraction measurements on the high-pressure product (PC55) were consistent with space group $P6_3/m$. It was noted earlier [14] that the response of the unit-cell parameters of apatite to accommodation of the carbonate ion is complex. In particular, substitution of OH^- by type A carbonate results in progressive increase in a and decrease in c [17,18], whereas substitution of phosphate by type B carbonate results in progressive decrease in a and increase in c [19,20]. Thus, the a parameter of our high-pressure CAp (xt376 in Table 1) corresponds with the type A calibration curve of Bonel [17], but the c parameter does not. Annealing at 1000°C resulted in progressive reduction in a with little change in c, giving unit-cell parameters in fair agreement with those for type A–B CAp synthesized at 0.55 kbar [11,12].

X-ray structure refinement of PC55 CAp started with the ideal structure of OHAp. It was evident from difference Fourier maps that the electron density in the apatite channel was very different from that of OHAp, and occupancy refinements of other OHAp positions suggested a deficiency of electron density at P and O(3) as well (Table 2). The refined CAp structure showed weak electron density at the positions O(H) (interpreted as a combination of minor OH or O, and one oxygen of the type A2 carbonate ion), O(A2) (interpreted as the other two oxygen atoms of the type A2 carbonate ion), C (at the origin), O(A11) and O(A12) (interpreted as the three oxygen atoms of the type A1 carbonate ion), and O(B3) (one oxygen of the type B carbonate ion). We emphasize that these features were all very weak in difference electron density maps, being equivalent in strength to H atoms with occupancies of 0.8, 0.5, 0.8, and 0.4 for O(A11), O(A12), O(A2), and O(B3), respectively, but the successive inclusion of each one in the structure resulted in a significant reduction in the R index (from 0.066 to 0.047, 0.041, 0.027, and 0.024, respectively). All of the carbonate oxygen atoms are in general positions and, therefore, are disordered with a multiplicity of twelve. The occupancies of O(A11) and O(A2) exceed 0.083 (i.e. 1/12), showing that these positions must each represent two non-equivalent oxygen atoms coalesced by symmetry repetition. More generally, overlap of electron density was particularly troublesome for channel atoms located near the c-axis [e.g. O(H), C, O(A11)] and for the type B carbonate ion oxygens near O(1) and O(2). Because of these limitations in resolution, it was not possible to refine simultaneously both occupancy and displacement parameters for atoms of the carbonate ions. Instead, an arbitrary isotropic displacement (thermal) parameter of value $U = 0.025$ was assigned to each of these atoms and the refinement was allowed to converge by varying the site occupancies. In addition, the occupancy of O(3) was constrained to $[1.0-(0.5-P)]$.

The configuration of the type A1 carbonate ion in PC55 is equivalent to that of type A carbonate in the $P\bar{3}$ structure. The carbonate ion is oriented with its plane and two of its oxygen atoms close to the c-axis, in the closed configuration (Fig. 1). O(A11) represents the two non-equivalent oxygen atoms close to the c-axis which are coalesced in the average structure due to symmetry repetition. The third oxygen, O(A12), is better resolved and, in agreement with the present reconstruction, has a refined occupancy of about one-half of that O(A11). The resulting O–O distances are 2.18, 2.22 and 1.92 Å, in reasonable agreement with the expected O–O distance (2.219 Å; 14). The observed C–O distances and O–C–O bond angles are meaningless on account of the poor resolution of the C atom, which is smeared about the origin by displacement and disorder of both types A1 and A2 carbonate ions. The type A2 carbonate ion is represented by two O(A2) atoms and O(H). It is, therefore, in the open vertical configuration [12], but tilted slightly away from the c-axis (Fig. 1). The O–O distances (2.17, 2.02 and 1.82 Å) are again reasonable, in view of overlap of the two O(A2) atoms and uncertainty in defining O(H). The apatite channel is interpreted to contain a mixed up (but, perhaps, locally ordered) sequence of types A1 and A2 carbonate ions and OH (or O) anions, as suggested in Fig. 1. Note that the apatite channel will only accommodate an excess of volatile anion groups if the types A1 and A2 carbonate ions and

OH are in a mixed up sequence, with the type A2 carbonate ion in the stuffed apatite channel location of substitution scheme (2a).

The presence of type B carbonate is revealed in the X-ray structure by the low occupancies of the P and O(3) positions [30], with a corresponding residual electron density at the location labelled O(B3) (Table 2; Fig. 2). The other two oxygen atoms of the type B carbonate ion are close to (and coalesced with) O(1) and O(2), respectively. The O–O distances (2.00, 2.28 and 2.51 Å) are not well defined, and the C atom was not resolved. However, it is clear that the type B carbonate ion is located close to the sloping faces of the PO_4 tetrahedron, in agreement with the conclusion of Elliott [7]. The accommodation of type B carbonate must result in considerable disruption of the CAp structure. In particular, the second O(3) atom of the substituted PO_4 group must be displaced away from the bonding sphere of the carbonate ion. These structural details, together with atom displacements in the wall of the CAp channel, are discussed in a separate study [31].

The X-ray reflection data for the structure analysis of PC55 were reduced using the empirical absorption procedure in SORTAV, which is based on comparison of equivalent reflections for the entire CCD data set indexed by the COLLECT software. A spherical crystal shape was assumed for the isotropic extinction correction. Space group $P6_3/m$ was uniquely indicated by SHELXTL/PC (combined-figure-of-merit = 2.00). The weighting procedure (w) used in the least-squares refinement was $w = 1/[\sigma^2_{(\mathrm{Fobs})} + (qF_{\mathrm{obs}})^2]$, where F_{obs} is the observed structure factor and $q = 0.015$. The low value of R, near-unit value of the goodness-of-fit parameter (Table 1), and insignificant number of reflections assigned zero intensity based on $I < 3\sigma_{(I)}$ and having $F_{\mathrm{calc}} > 10$ (Fig. 4a), show that the present structure adequately accounts for the X-ray diffraction pattern of the quenched high-pressure type A–B CAp product. Study of crystals synthesized at high pressure from a more $CaCO_3$-rich starting mixture [31] has resulted in a similar structure for type A–B CAp, providing independent confirmation of the three structurally distinct locations for the carbonate ion. The maximum and minimum residual electron densities (Table 1) were located near Ca(2). Local displacements of Ca(2) were anticipated to optimize Ca(2)–(O,OH) bond distances in the disordered structure but were at and beyond the limit of resolution of the structure analysis. Furthermore, the complexly disordered structural elements (carbonate, phosphate and hydroxyl ions, and vacancies) and lack of precise information on local stereochemical environments did not seem to warrant further confirmation of the type A–B CAp structure from bond valence calculation.

The X-ray structures of type A–B CAp annealed in air for 15 min (PC55-1000-15; xt383) and 12 h (PC55-1000-12; xt377; Tables 1–3) were broadly similar to that of the unannealed material. The structure refinements of xt383 and xt377 were made in space group $P6_3/m$, using the above procedures but with $q = 0$ in the weighting scheme. The progressive increases in the values of R and R_{w} and in standard deviations of structural parameters show that the resolution of structural features decreases progressively with increasing annealing time, probably reflecting progressive local re-crystallization of the CAp. Re-crystallization (and secondary crystallization, in particular) degrades the diffraction quality of crystals and complicates the correspondence between the "average" structure and the actual structural state of the apatites. These effects are also reflected in the marked increase in the number of "unobserved" reflections with significant values for F_{calc} (Fig. 4b).

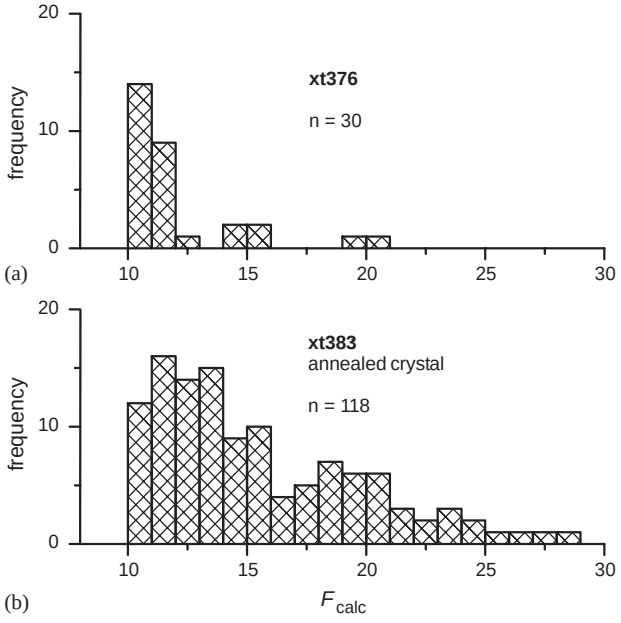

Fig. 4. Frequency distribution for reflections assigned zero intensity based on $I < 3\sigma_{(I)}$ and having $F_{\mathrm{calc}} > 10$, showing marked deterioration in diffraction quality of type A–B CAp after annealing at 1000°C for 15 min (xt383; PC55-1000-15). Note that $F_{\mathrm{calc}} = 10$ corresponds to only 0.3% of the maximum value of $(F_{\mathrm{calc}})^2$.

The formula amounts of the three structurally distinct carbonate ions in the high-pressure synthesized and annealed CAp are compared in Table 4. The formula amount of type A1 carbonate is the x compositional variable and that of type B is y of the schematic formula (2b). Formula amounts for the X-ray structure method represent refined electron densities. The electron density of O(A12) has been used to estimate the formula amount of type A1 carbonate, because this off-axis carbonate atom is better resolved than O(A11) and free of assumptions used to refine the overlapped electron density for atoms close to the c-axis. The electron density of O(B3) has been used for type B carbonate, and one-half of that of the off-axis O(A2) for type A2

carbonate. Formula amounts of types B and A2 carbonate from FTIR spectroscopy (Fig. 3) have been calculated by normalizing peak areas against the X-ray structure result for the type A1 carbonate. We emphasize that the presently proposed structure for type A–B CAp synthesized at 3 GPa and quenched to 1 bar is based solely on the single-crystal X-ray structure analysis of sample PC55. The X-ray structures for the two annealed CAp samples are of lesser quality but, nevertheless, are similar to that of PC55. The FTIR spectra show that types A1 and B carbonate in CAp synthesized at high-pressure are equivalent to types A and B carbonate in low-pressure apatites and bone and enamel, whereas moderate amounts of type A2 carbonate is a high-pressure feature. Also, the progressive diminution in the strength of the A2 absorption bands (Fig. 3) is consistent with the selective loss of this carbonate ion species in CAp annealed at low pressure.

The amount of type A2 carbonate is approximately one-half of that of type B in the two annealed CAp structures, consistent with the substitution scheme (2a) and the solid solution formula $Ca_{10}(PO_4)_{6-y}(CO_3)_{x+(3/2)y}(OH)_{2-2x}$, with $x \sim 0.7$, $y \sim 0.6$. Therefore, we conclude that the structural role of type A2 carbonate here is to charge compensate CO_3^{2-} for PO_4^{3-} substitution, in the absence of other charge compensating mechanisms. The amount of type A2 carbonate in the quenched high-pressure CAp (PC55) is in excess of $y/2$ (Table 4), possibly indicating added complexity in the form of substitution of type A2 carbonate for channel hydroxyl or O^{2-}. It appears that the carbonate ion is forced into the stuffed channel position in high-pressure synthesis. It is significant that type A2 carbonate is readily lost on annealing at high temperature in air. Both of the crystals xt383 and xt377 showed weak intensity for the 0 0 3 reflection in violation of $P6_3/m$ symmetry, although the intensity of $h\,k\,\ell$, $h\,k\,\bar{\ell}$ reflection pairs remain identical within error of measurement. This suggests that loss of the type A2 carbonate is associated with some domain ordering of the type A1 carbonate ion within the apatite channel, in the manner of the $P\bar{3}$ structure [14] but with domains in twin orientation. Given this evidence for mobility of the channel constituents, it is possible that the actual high-pressure structure of PC55 CAp may have been modified during quenching of the synthesis experiment.

The present positions of the types A1 and B carbonate ions differ from those of two recent X-ray structure studies [12,13]. It is possible that the structures of other preparations of CAp and C–OHAp are more complicated than presently proposed. However, the IR spectrum for types A–B CAp in Suetsugu et al. [12] and Raman data for type B C–OHAp in Ivanova et al. [13] are consistent with the present and other literature studies and it seems unlikely that different stereochemical environments would result in essentially the same vibrational spectrum for any given type of carbonate ion. The present location for the type A1 carbonate ion is well established by our $P\bar{3}$ structure [14]. Suetsugu et al. [11,12] did not investigate the possibility that their crystal symmetry might be twinned $P\bar{3}$, and their thermal parameters for the off-axis carbonate oxygens are too large for meaningful refinement of the type A1 carbonate ion. The type B carbonate ion was located in Ivanova et al. [13] by Rietveld refinement of X-ray powder diffraction data, giving a structure of lower resolution than PC55 (xt376; Table 2). There seems little advantage to continuing the refinement of the PC55 structure with the carbonate ions constrained to ideal geometry, since all resolved electron density associated with the carbonate ions is already accounted for in the present unconstrained refinement.

Acknowledgments

We thank three reviewers for comments on the manuscript, Michael Jennings for collection of the X-ray reflection data, Penny King for use of high-pressure and FTIR facilities, and the Natural Sciences and Engineering Research Council of Canada for financial support.

References

[1] P.E. Mackie, R.A. Young, J. Appl. Crystallogr. 6 (1973) 26–31.
[2] J.M. Hughes, M. Cameron, K.D. Crowley, Am. Miner. 74 (1989) 870–876.
[3] J.C. Elliott, in: E. Brès, P. Hardouin (Ed.), Les matériaux en phosphate de calcium, Aspects fondamentaux, Sauramps Medical, Montpellier, 1998, p. 25.
[4] J.M. Hughes, J. Rakovan, in: M.J. Kohn, J. Rakovan, J.M. Hughes (Eds.), Phosphates, Rev. Miner. Geochem., Vol. 48, Miner. Soc. Am., Washington, DC, 2002, p. 1.
[5] Y. Pan, M.E. Fleet, in: M.J. Kohn, J. Rakovan, J.M. Hughes (Eds.), Phosphates, Rev. Miner. Geochem., Vol. 48, Miner. Soc. Am., Washington, DC, 2002, p. 13.
[6] J.C. Elliott, Structure and Chemistry of the Apatites and Other Calcium Orthophosphates, Elsevier, Amsterdam, 1994.
[7] J.C. Elliott, in: R.W. Fearnhead, M.V. Stack (Eds.), Tooth Enamel, John Wright & Sons, Bristol, UK, 1964, p. 20.
[8] K. Beshah, C. Rey, M.J. Glimcher, M. Schimizu, R.G. Griffin, J. Solid State Chem. 84 (1990) 71–81.
[9] P. Regnier, A.C. Lasaga, R.A. Berner, O.H. Han, K.W. Zilm, Am. Miner. 79 (1994) 809–818.
[10] P. Comodi, Y. Liu, Eur. J. Miner. 12 (2000) 965–974.
[11] Y. Suetsugu, I. Shimoya, J. Tanaka, J. Am. Ceram. Soc. 81 (1998) 746–748.
[12] Y. Suetsugu, Y. Takahashi, F.P. Okamura, J. Tanaka, J. Solid State Chem. 155 (2000) 292–297.
[13] T.I. Ivanova, O.V. Frank-Kamenetskaya, A.B. Kol'tsov, V.L. Ugolkov, J. Solid State Chem. 160 (2001) 340–349.
[14] M.E. Fleet, X. Liu, J. Solid State Chem. 174 (2003) 412–417.
[15] Siemens, SHELXTL PC. Version 4.1, Siemens Analytical X-ray Instruments, Inc., Madison, WI, USA, 1993.

[16] J.A. Ibers, W.C. Hamilton (Eds.), International Tables for X-ray Crystallography, Vol. IV, Kynoch Press, Birmingham, UK, 1974.
[17] G. Bonel, Ann. Chim. 7 (1972) 65–87.
[18] R.Z. LeGeros, O.R. Trautz, E. Klein, J.P. LeGeros, Experimentia 25 (1969) 5–7.
[19] D.G.A. Nelson, J.D.B. Featherstone, Calcif. Tissue Int. 34 (1982) S69–S81.
[20] M. Vignoles, G. Bonel, D.W. Holcomb, R.A. Young, Calcif. Tissue Int. 43 (1988) 33–40.
[21] J.C. Elliott, in: M.J. Kohn, J. Rakovan, J.M. Hughes (Eds.), Phosphates, Rev. Miner. Geochem., Vol. 48, Miner. Soc. Am., Washington, DC, 2002, p. 427.
[22] W.B. White, in: V.C. Farmer (Ed.), The Infrared Spectra of Minerals, Mono. 4, Miner. Soc., London, 1974, p. 227.
[23] T. Tyliszcak, BAN Data Analysis Program, McMaster University, 1992.
[24] S. Shimoda, T. Aoba, E.C. Moreno, Y. Miake, J. Dent. Res. 69 (1990) 1731–1740.
[25] R.V. Santos, R.N. Clayton, Am. Miner. 80 (1995) 336–344.
[26] Y. Miyamoto, K. Ishikawa, M. Takechi, T. Toh, Y. Yoshida, M. Nagayama, M. Kon, K. Asaoka, J. Biomed. Mater. Res. 37 (1997) 457–464.
[27] J. Barralet, S. Best, W. Bonfield, J. Biomed. Mater. Res. 41 (1998) 79–86.
[28] R.G.J. Strens, in: V.C. Farmer (Ed.), The Infrared Spectra of Minerals, Mono. 4, Miner. Soc., London, 1974, p. 305.
[29] S.E.P. Dowker, Infrared spectroscopic studies of thermally treated carbonate-containing apatites, Ph.D. Thesis, University of London, UK, 1980.
[30] R.M. Wilson, J.C. Elliott, S.E.P. Dowker, Am. Miner. 84 (1999) 1406–1414.
[31] M.E. Fleet, X. Liu, P.L. King, Am. Miner., reviewed.